

Elliptical instability of a rapidly rotating, strongly stratified fluid

J M Aspden and J Vanneste

School of Mathematics and Maxwell Institute for Mathematical Sciences
University of Edinburgh, Edinburgh EH9 3JZ, UK

The elliptical instability of a rotating stratified fluid is examined in the regime of small Rossby number and order-one Burger number corresponding to rapid rotation and strong stratification. The Floquet problem describing the linear growth of disturbances to an unbounded, uniform-vorticity elliptical flow is solved using exponential asymptotics. The results demonstrate that the flow is unstable for arbitrarily strong rotation and stratification; in particular, both cyclonic and anticyclonic flows are unstable. The instability is weak, however, with growth rates that are exponentially small in the Rossby number. The analytic expression obtained for the growth rate elucidates its dependence on the Burger number and on the eccentricity of the elliptical flow. It explains in particular the weakness of the instability of cyclonic flows, with growth rates that are only a small fraction of those obtained for the corresponding anticyclonic flows. The asymptotic results are confirmed by numerical solutions of Floquet problem.

1 Introduction

Elliptical instability, the three-dimensional instability of two-dimensional flows with elliptical streamlines, has been the focus of a great deal of research activity. The review by Kerswell¹ discusses the main results up to 2002 and emphasises the relevance of elliptical instability to a broad range of applications. One of these is the instability of two-dimensional vortices that are deformed elliptically by a large-scale strain flow. This is especially important for the dynamics of the atmosphere and ocean, since this is characterised by an abundance of vortices that are deformed through either mutual interactions or the effect of large-scale flows. In this context, however, the planetary rotation and density stratification need to be taken into account.

Rotation and stratification clearly exert a strong influence on elliptical instability: since this stems from the parametric resonance between the periodic fluctuations associated with

the elliptical motion and the free waves supported by the flow, the dispersion relation of these waves is critical. In the presence of rotation and stratification, the waves are inertia-gravity waves whose frequency is bounded from below by the minimum of the Coriolis parameter f and Brunt–Väisälä frequency N . As a consequence, a vortex of fixed vorticity ceases to be unstable by the subharmonic instability responsible for the simplest form of elliptical instability when f and N exceeds a certain threshold. As these parameters increase further, instabilities are limited to resonances of higher and higher order, leading to decreasing growth rates. This was clearly demonstrated by Miyazaki² on the basis of numerical solutions of the Floquet problem that models elliptic instability. Further numerical results were obtained by McWilliams and Yavneh³ who concentrated on the regime of rapid rotation and strong stratification with $N > f$ most relevant to the atmosphere and ocean. Their broad motivation was the role that instabilities play in the generation of inertia-gravity-wave-like motion, and the resulting breakdown of the nearly geostrophic and hydrostatic balance that is typical of much of the atmosphere and ocean. The present paper shares the same motivation. It re-examines the elliptical instability of a rotating stratified fluid and derives explicit analytical results in the limit of fast rotation $f \gg \Omega$ and strong stratification $N \gg \Omega$, where Ω denotes the (relative) vorticity of the flow.

Several recent papers^{4;5;6;7} have demonstrated in specific examples that instabilities of well-balanced basic flows to inertia-gravity-wave perturbations (or perturbations related to similar fast waves) have growth rates that are exponentially small in the Rossby number, here proportional to $\Omega/f \ll 1$.¹ Theoretical arguments^{8;9} indicate that this is a generic property, and the elliptical instability examined in this paper is no exception. In this case, the exponential smallness can be roughly understood by noting that, in the manner typical of parametric instabilities¹⁰, the growth rates of the elliptical instability can be expected to be proportional to Ω^n , where n is the order of the resonance. Since, as pointed out by Miyazaki², the minimum n is of the order f/Ω (for $N > f$), this leads to the conclusion that growth rates are beyond all orders in the Rossby number. To go further than this rough argument and provide an estimate for the growth rate requires the exponential-asymptotics analysis of the Floquet problem relevant to the elliptical instability. We carry out this analysis and, rather than relying on general asymptotic results for Hill's equations¹¹, directly relate the growth of solutions to the occurrence of a Stokes phenomenon¹² which we capture using a combination of WKB expansion and matched asymptotics in complex time. The analytical results are confirmed by the numerical solutions of the Floquet problem.

¹Note that we use the conventional form of Rossby number rather than its inverse as used in Ref.².

One of the issues which our treatment clarifies is the difference between the instability of cyclonic and anticyclonic vortices. Cyclones have been recognised as less unstable than anticyclones, to the extent that McWilliams and Yavneh³ considered only the instability of the latter. We show that the cyclones are in fact linearly unstable, with growth rates that have the same exponential dependence on the Rossby number as the corresponding anticyclones but differ by a factor which, although formally of order one, turns out to be numerically very small.

The plan of this paper is as follows. In section 2, we formulate the problem of elliptical instability in a rotating stratified fluid modelled using the Boussinesq approximation. We use the simplest instance of elliptical instability, that of an unbounded elliptical vortex with uniform vorticity. This makes it possible to seek global solutions in the form of plane waves with time-periodic wavevector and an amplitude that satisfies a Hill's equation. (Results for this particular case have a much broader appeal, however, since an identical Hill's equation arises when the stability of more general elliptical vortices is examined locally using the geometric-optics technique.^{13;14}) The Floquet problem associated with the Hill's equation is solved asymptotically in section 3 in the limit of fast rotation and strong stratification, with the eccentricity of the elliptical streamlines assumed of order one. For simplicity, we also make the hydrostatic approximation assuming that $N \gg f$ and an order-one Burger number. The asymptotic derivation is only sketched in section 3, with technical details relegated to Appendix A. The asymptotic results are confirmed by direct numerical solution of the Floquet problem in section 4. The effect of a finite N/f is also briefly examined there.

2 Formulation

We consider the stability of a horizontal elliptical flow in a three-dimensional stratified fluid, with constant Brunt–Väisälä frequency N , rotating about the vertical axis at rate $f/2 > 0$. The flow's streamfunction, velocity and vorticity are written as

$$\Psi = -\frac{1}{2}(bx^2 + ay^2), \quad \mathbf{U} = (ay, -bx, 0) \quad \text{and} \quad \Omega = a + b, \quad (2.1)$$

where $ab > 0$. We define

$$\varsigma = \text{sgn } a = \text{sgn } b$$

and note that the flow is anticyclonic for $\varsigma = 1$, and cyclonic for $\varsigma = -1$. Three dimensionless parameters characterise the flow, namely

$$e = \sqrt{a/b}, \quad \epsilon = \sqrt{ab}/f \quad \text{and} \quad f/N, \quad (2.2)$$

which are recognised as the aspect ratio of the elliptical flow, a Rossby number and the Prandtl ratio. We assume that $e > 1$ without loss of generality.

Perturbations to the flow (2.1) take the form of plane waves with time-dependent wavevector, with each field written as

$$u(\mathbf{x}, t) = \hat{u}(t)e^{i\mathbf{k}(t)\cdot\mathbf{x}},$$

where the wavevector $\mathbf{k} = (k, l, m)$ satisfies

$$\dot{k} = bl, \quad \dot{l} = -ak \quad \text{and} \quad \dot{m} = 0, \quad (2.3)$$

the overdot denoting differentiation with respect to t . In what follows, we use a dimensionless time variable obtained by taking $(ab)^{-1/2}$ as a reference time. In terms of this variable, the solutions to (2.3) have the simple form

$$k = k_0 \cos t, \quad l = -\zeta e k_0 \sin t \quad \text{and} \quad m = m_0, \quad (2.4)$$

where k_0 and m_0 are constant. The stability of (2.1) depends on the behaviour of the amplitudes $\hat{u}(t)$, $\hat{v}(t)$, etc. as $t \rightarrow \infty$. These satisfy a set of ordinary differential equations with time-periodic coefficients. Following McWilliams and Yavneh³, this set can be conveniently reduced to a single second-order equation for the amplitude of the vertical component of the vorticity $\hat{\zeta} = i(l\hat{v} - k\hat{u})$. Assuming that the perturbation potential vorticity vanishes, this equation reduces to

$$\ddot{\zeta} + \frac{2\zeta k l m^2 (e - e^{-1})}{\kappa^2 (k^2 + l^2)} \dot{\zeta} + \frac{1}{\epsilon^2} \left[(1 - \zeta \epsilon (e + e^{-1})) \left(1 - \frac{2\zeta \epsilon e k_0^2}{k^2 + l^2} \right) \frac{m^2}{\kappa^2} + \frac{N^2 (k^2 + l^2)}{f^2 \kappa^2} \right] \zeta = 0, \quad (2.5)$$

where $\kappa^2 = k^2 + l^2 + m^2$ and we have omitted the hat on the amplitude ζ . Four dimensionless parameters appear in this equation: the three flow parameters (2.2), and the initial aspect ratio m_0/k_0 of the perturbation. Note that anticyclonic flows (with $\zeta = 1$) are susceptible to centrifugal instability (e.g. Ref.¹⁵) when the relative vorticity exceeds f , that is, for $\epsilon(e + e^{-1}) > 1$. Since we focus on the regime $\epsilon \ll 1$ we do not consider this instability further.

Most of this paper focuses on a limiting case of (2.5) obtained by making the hydrostatic approximation. This assumes that $m_0 \gg k_0$ and $N \gg f$ while

$$\mu = \frac{f m_0}{N k_0} = O(1). \quad (2.6)$$

This is the regime most relevant to the dynamics of the atmosphere and oceans since the condition $N \gg f$ is verified while, as we demonstrate below, the largest growth rates of the elliptical instability correspond to $\mu = O(1)$. The parameter μ can be recognised as the inverse

square root of a Burger number; it can be interpreted as the aspect ratio of the perturbation scaled by f/N as is natural in rapidly rotating, strongly stratified fluids.

In the hydrostatic approximation, κ^2 is approximated by m^2 , and (2.5) reduces to

$$\ddot{\zeta} + \frac{2\zeta kl(e - e^{-1})}{k^2 + l^2} \dot{\zeta} + \frac{1}{\epsilon^2} \left[(1 - \zeta\epsilon(e + e^{-1})) \left(1 - \frac{2\zeta\epsilon\epsilon k_0^2}{k^2 + l^2} \right) + \frac{N^2(k^2 + l^2)}{f^2 m^2} \right] \zeta = 0. \quad (2.7)$$

Using (2.4) and defining $\psi > 0$ by

$$e^2 = 1 + \psi^2, \quad (2.8)$$

we rewrite this equation as

$$\ddot{\zeta} - p(t)\dot{\zeta} + \frac{1}{\epsilon^2} [\omega^2(t) - \epsilon q(t) + \epsilon^2 r(t)] \zeta = 0. \quad (2.9)$$

Here

$$\omega^2 = 1 + \frac{N^2(k^2 + l^2)}{f^2 m^2} = 1 + \mu^{-2}(1 + \psi^2 \sin^2 t), \quad (2.10)$$

can be recognised as the square of the inertia-gravity-wave frequency (non-dimensionalised by f). We have also introduced

$$p(t) = \frac{\psi^2 \sin(2t)}{1 + \psi^2 \sin^2 t}, \quad q(t) = \zeta \left(e + e^{-1} + \frac{2e}{1 + \psi^2 \sin^2 t} \right) \quad \text{and} \quad r(t) = \frac{2(e^2 + 1)}{1 + \psi^2 \sin^2 t}. \quad (2.11)$$

Equation (2.9) is a Hill equation, with coefficients that are π -periodic in t . Its stability is determined using the Floquet theory for Hill equations¹⁰. Briefly, if $\zeta(t) = (\zeta_1(t), \zeta_2(t))^T$ is a column vector of independent solutions,

$$\zeta(t + \pi) = M\zeta(t)$$

for some constant matrix M . The eigenvalues λ of M are then the Floquet multipliers, and two fundamental solutions can be found for which

$$\zeta(t) = e^{\sigma t} \phi(t), \quad (2.12)$$

where

$$\sigma = \frac{1}{\pi} \log \lambda \quad (2.13)$$

is the Floquet exponent, and $\phi(t)$ is π -periodic. Note that the form of the coefficient of $\dot{\zeta}$ ensures that the two multipliers satisfy $\lambda_1 \lambda_2 = 1$. Instability occurs when one of these is such that $|\lambda| > 1$ or, equivalently, $\text{Re } \sigma > 0$. The matrix M is computed by relating ζ and $\dot{\zeta}$ at two times t and $t + \pi$. Here we choose $t = -\pi/2$ and compute M as

$$M = [\zeta(\pi/2), \dot{\zeta}(\pi/2)][\zeta(-\pi/2), \dot{\zeta}(-\pi/2)]^{-1}. \quad (2.14)$$

Our aim is to determine the largest values of the growth rate $\text{Re } \sigma$ for (2.9) analytically in the fast-rotation regime $\epsilon \ll 1$, with $N \gg f$, $\mu = O(1)$ and $\psi = O(1)$. In this regime (2.9) resembles the Hill equations with large parameters whose stability has been studied by Weinstein and Keller¹¹ using a mapping to parabolic cylinder functions. However, there are difficulties in applying their results directly, related to the presence of a first derivative term that is singular for the complex values of t such that $k^2 + l^2 = 0$. We have therefore found it simpler to develop a different approach, combining WKB analysis with complex-time matching. This approach, which has the advantage of demonstrating the link between the instability and the Stokes phenomenon^{12;16}, is described in the next section and in Appendix A. The analytic results obtained there are confirmed and extended to finite N/f in section 4 by solving (2.9) numerically.

3 WKB analysis

A WKB solution of the form

$$\zeta = A(t)e^{i\theta(t)/\epsilon} \quad (3.1)$$

can be introduced into (2.9), and the (real) functions $A(t)$ and $\theta(t)$ can be derived by expansion in powers of ϵ . At leading order, we find that

$$\theta_0(t) = \int_{-\pi/2}^t \omega(t') dt'. \quad (3.2)$$

At the next order, we have

$$\frac{\dot{A}_0}{A_0} = -\frac{\dot{\omega}}{2\omega} + \frac{p}{2}, \quad (3.3)$$

$$\dot{\theta}_1 = -\frac{q}{2\omega}. \quad (3.4)$$

We note that $A_0(t)$ is π -periodic; this is also true for higher-order corrections, so that there is no instability to any algebraic order in ϵ : the fundamental solutions are given by ζ in (3.1) and its complex conjugate, and the Floquet multipliers are simply $\lambda = \pm \exp(i\theta(\pi/2))$ (taking $\theta(-\pi/2) = 0$). Instability is necessarily an exponentially small effect; furthermore, it can only occur for values of the parameters such that λ is exponentially close to ± 1 . This is because the condition for instability $|\lambda| > 1$ requires the two multipliers to be purely real; however, they are complex conjugate to all orders in ϵ , a property which persists in the presence of a small perturbation in the non-degenerate cases $\lambda \neq \pm 1$.

Computations detailed below show that the solution defined by (3.1) for $-\pi/2 \leq t < -\delta$, with $\delta \ll 1$, switches on an exponentially small term as the Stokes line $\operatorname{Re} t = 0$ is crossed. Denoting by S the corresponding Stokes multiplier, which is exponentially small in ϵ , this implies that the pair of solution

$$\zeta = A(t)e^{i\theta(t)/\epsilon} \quad \text{and} \quad \bar{\zeta} = A(t)e^{-i\theta(t)/\epsilon} \quad (3.5)$$

valid for $-\pi/2 \leq t < -\delta$ (for some $\epsilon^{1/2} \ll \delta \ll 1$) becomes

$$\zeta = A(t) \left[e^{i\theta(t)/\epsilon} + S e^{-i\theta(t)/\epsilon} \right] \quad \text{and} \quad \bar{\zeta} = A(t) \left[e^{-i\theta(t)/\epsilon} + \bar{S} e^{i\theta(t)/\epsilon} \right] \quad (3.6)$$

for $\delta < t \leq \pi/2$. Taking $\zeta = (\zeta, \bar{\zeta})^T$, we compute the matrix M in (2.14). We first have that

$$[\zeta(\pi/2), \dot{\zeta}(\pi/2)] = \begin{pmatrix} A(e^{i\theta/\epsilon} + S e^{-i\theta/\epsilon}) & (i\epsilon^{-1}\dot{\theta}A + \dot{A})e^{i\theta/\epsilon} + S(-i\epsilon^{-1}\dot{\theta}A + \dot{A})e^{-i\theta/\epsilon} \\ A(e^{-i\theta/\epsilon} + \bar{S}e^{i\theta/\epsilon}) & (-i\epsilon^{-1}\dot{\theta}A + \dot{A})e^{-i\theta/\epsilon} + \bar{S}(i\epsilon^{-1}\dot{\theta}A + \dot{A})e^{i\theta/\epsilon} \end{pmatrix},$$

where A, \dot{A}, θ and $\dot{\theta}$ are evaluated at $t = \pi/2$. Similarly,

$$[\zeta(-\pi/2), \dot{\zeta}(-\pi/2)] = \begin{pmatrix} A & i\epsilon^{-1}\dot{\theta}A + \dot{A} \\ A & -i\epsilon^{-1}\dot{\theta}A + \dot{A} \end{pmatrix}.$$

Here A, \dot{A} and $\dot{\theta}$ can be evaluated at $t = \pi/2$, as above, since their values at $t = \pm\pi/2$ coincide. Computing (2.14) gives the simple result

$$M = \begin{pmatrix} e^{i\theta/\epsilon} & S e^{-i\theta/\epsilon} \\ \bar{S} e^{i\theta/\epsilon} & e^{-i\theta/\epsilon} \end{pmatrix}. \quad (3.7)$$

Here $\theta = \theta(\pi/2)$ or, more generally, $\theta = \theta(\pi/2) - \theta(-\pi/2)$ which accommodates any convention for the arbitrary choice of $\theta(-\pi/2)$.

Suppose now that the parameters are such that

$$e^{i\theta/\epsilon} = \pm(1 + iT) + O(T^2) \quad (3.8)$$

for some $T \in \mathbb{R}$ of a similar order of magnitude as S . The Floquet multipliers obtained from (2.14) are then given by

$$\lambda = \pm \left(1 + \sqrt{|S|^2 - T^2} \right) + O(|S|^2) \quad \text{and} \quad \lambda = \pm \left(1 - \sqrt{|S|^2 - T^2} \right) + O(|S|^2). \quad (3.9)$$

Clearly, one of these multipliers satisfies $|\lambda| > 1$, and the flow is unstable, provided that $-|S| \leq T \leq |S|$, that is, in exponentially narrow instability bands. The corresponding growth rate

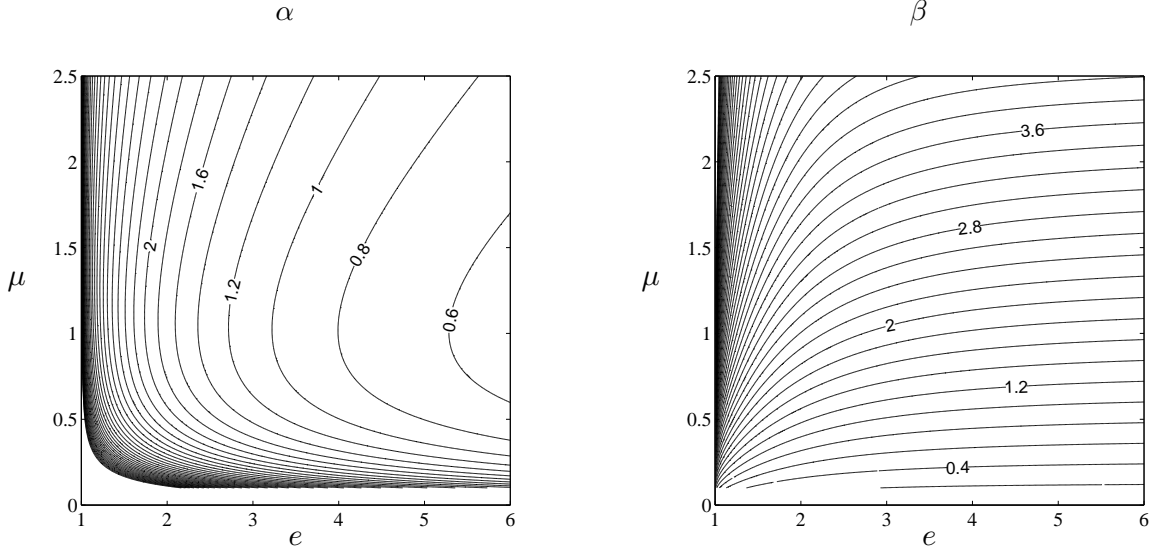


Figure 1: Parameters α and β governing the maximum growth rates according to (3.10)–(3.11) as functions of e and μ .

$\sigma = \sqrt{|S|^2 - T^2}/\pi + O(|S|^2)$ is maximum at the centre of these bands, for $T = 0$, and is given by

$$\sigma_{\max} \sim \frac{|S|}{\pi}. \quad (3.10)$$

The computation of S is carried out in Appendix A. There we show that

$$|S| = e^{-\alpha/\epsilon + \beta}, \quad (3.11)$$

where

$$\alpha = \frac{2}{\mu} \int_0^{\sqrt{1+\mu^2}/\psi} \sqrt{\frac{1+\mu^2-\psi^2 x^2}{1+x^2}} dx \quad \text{and} \quad (3.12)$$

$$\beta = \mu \mathcal{f} \int_0^{\sqrt{1+\mu^2}/\psi} \left(e + e^{-1} + \frac{2e}{1-\psi^2 x^2} \right) \frac{dx}{\sqrt{(1+\mu^2-\psi^2 x^2)(1+x^2)}}. \quad (3.13)$$

Here \mathcal{f} denotes the Cauchy principal value of the integral, whose integrand is singular at $x = 1/\psi$.

Figure 1 shows the values of α and β as functions of e and μ . Some conclusions can be drawn from the figure and the examination of the explicit expressions (3.12)–(3.13). First, $\alpha \rightarrow \infty$ in the limits of both small and large μ ; specifically $\alpha = O(\mu^{-1})$ as $\mu \rightarrow 0$ and $\alpha = O(\log \mu)$ as $\mu \rightarrow \infty$. This suggests, as is confirmed by Figure 1, that the largest growth rates are attained for $\mu = O(1)$. Thus, the aspect ratio of the perturbations that grow as a result of the elliptical instability of vortices should be expected to be the Prandtl ratio: $m_0/k_0 = O(N/f)$. Second,

the behaviour of α for small and large eccentricity is given by

$$\alpha \sim -\frac{2\sqrt{1+\mu^2}}{\mu} \left(\log \psi + 1 - 2 \log 2 - \frac{1}{2} \log(1 + \mu^2) \right) \quad \text{as } \psi \rightarrow 0, \quad (3.14)$$

$$\alpha \sim \frac{(1 + \mu^2)\pi}{2\mu\psi} \quad \text{as } \psi \rightarrow \infty. \quad (3.15)$$

The large- ψ expression (3.15) can actually be used to estimate α for values of ψ as small as 1, which makes it very useful. (For $\mu = 1$, for instance, the error in (3.15) is 15%, 10% and 5% for $\psi = 1, 1.5$ and 2 , respectively.) This expression shows in particular that the largest growth rates are attained precisely for $\mu \sim 1$ when ψ is large. Third, the obvious fact that $\beta > 0$ shows that anticyclonic flows ($\zeta = 1$) are more unstable than cyclonic flows ($\zeta = -1$). According to (3.11), the growth rate in an anticyclonic flow is a factor $\exp(2\beta)$ larger than the growth rate of the corresponding cyclonic flow. Formally, this is an $O(1)$ factor, but the typical values of β are such that it is numerically very small, so that the instability of cyclones is exceedingly weak and probably negligible in most circumstances. Note that because β is a decreasing function of e , the asymmetry between cyclones and anticyclones is the largest for small eccentricity.

The formulas (3.10)–(3.13) give completely explicitly expressions for the maximum growth rates of the elliptical instability in terms of the three parameters ϵ , μ and e (recall that $\psi = \sqrt{e^2 - 1}$). These growth rates are achieved when the three parameters are related in such a way that $\exp(i\theta/\epsilon) = \pm 1$, that is,

$$\theta = n\pi\epsilon, \quad n = 1, 2, \dots \quad (3.16)$$

This condition can be recognised as a resonance condition between the phase of the inertia-gravity oscillations and the period of rotation around the elliptical vortex (2π in the dimensionless time used here).

The growth rates can be written more directly in terms of ϵ , μ and e by solving (3.16) perturbatively, with $\theta = \theta_0 + \epsilon\theta_1 + \dots$, and θ_0 and θ_1 obtained from (3.2) and (3.4). This gives the approximate position of the instability bands as well as their width. To leading order, the instability bands are centred at values of e and μ satisfying

$$\theta_0 = \frac{1}{\mu} \int_{-\pi/2}^{\pi/2} \sqrt{1 + \mu^2 + \psi^2 \sin^2 t} dt = \frac{2}{\mu} \int_0^1 \sqrt{\frac{1 + \mu^2 + \psi^2 x^2}{1 - x^2}} dx = n\pi\epsilon, \quad n = 1, 2, \dots \quad (3.17)$$

The computation of the correction $\epsilon\theta_1$ is more involved. Note that it is in principle needed to obtain a leading-order approximation to the growth rate $\text{Re}\sigma$ as a function of e and μ . This is because the error on α needs to be $o(\epsilon)$, which requires to approximate the resonance values of e and μ with an $o(\epsilon)$ error also. We do not pursue these detailed computations here:

since the values of e and μ satisfying the resonance condition (3.16) are ϵ -close together, (3.10) provides a useful approximation to the growth rates of the instability without the need to locate the resonances accurately. This is demonstrated in the next section where we compare the prediction (3.10) with numerical solutions of the Floquet problem associated with (2.7).

Note that the band width can be deduced directly from the expression (3.17) for θ_0 . For fixed ϵ and e , for instance, T in (3.8) can be written as $T = \epsilon^{-1} \Delta\mu \partial_\mu \theta$, where $\Delta\mu$ is the distance between μ and the resonant values, and the derivative is evaluated at resonance. According to (3.9), the instability-band width is therefore $\Delta\mu = 2\epsilon|S|/\partial_\mu \theta$ where θ can be approximated by θ_0 .

4 Comparison with numerical results

We have solved the Floquet problem associated with equation (2.9) for the amplitude ζ numerically using Matlab's standard Runge–Kutta solver. The growth rates $\text{Re } \sigma$ obtained in this manner are compared with the asymptotic estimate (3.10) for σ_{\max} . To emphasise the exponential dependence on the inverse Rossby number $1/\epsilon$, it is convenient to display $\text{Re } \sigma$ as a function of $1/\epsilon$ for fixed values of μ and of e . Figure 2 shows the results obtained in case of anticyclonic vortices (with $\varsigma = 1$) for several values of e and μ . Similar results for cyclonic vortices ($\varsigma = -1$) are displayed in Figure 3.

The figures confirm the validity of our asymptotic estimate. They also suggest that this estimate remains useful for moderately small values of ϵ , say $\epsilon \lesssim 1/2$. Note that the dimensional growth rates are obtained by multiplying σ by \sqrt{ab} which is related to the relative vorticity $\Omega = a + b$ of the flow by $\sqrt{ab} = \Omega/(e + e^{-1})$. As expected from our asymptotics, the growth rates in the case of cyclonic flows are exceedingly small for $\epsilon \ll 1$ even for the large eccentricities used in Figure 3. Nonetheless, our results clarify the fact that all elliptical flows are unstable, regardless of the sense of the rotation, of its strength, and of the strength of the stratification. Note that the match between asymptotic and numerical results for cyclonic flows appears to degrade for small ϵ (i.e., large $1/\epsilon$); this is because the smallness of both the growth rate and instability-band width makes the maximum growth rate delicate to estimate numerically.

The separation between instability bands can be estimated from the asymptotic formula (3.17): in terms of the varying $1/\epsilon$ used in the figures, it is given by

$$\gamma = \frac{\pi\mu}{2 \int_0^1 \sqrt{\frac{1 + \mu^2 + \psi^2 x^2}{1 - x^2}} dx}.$$

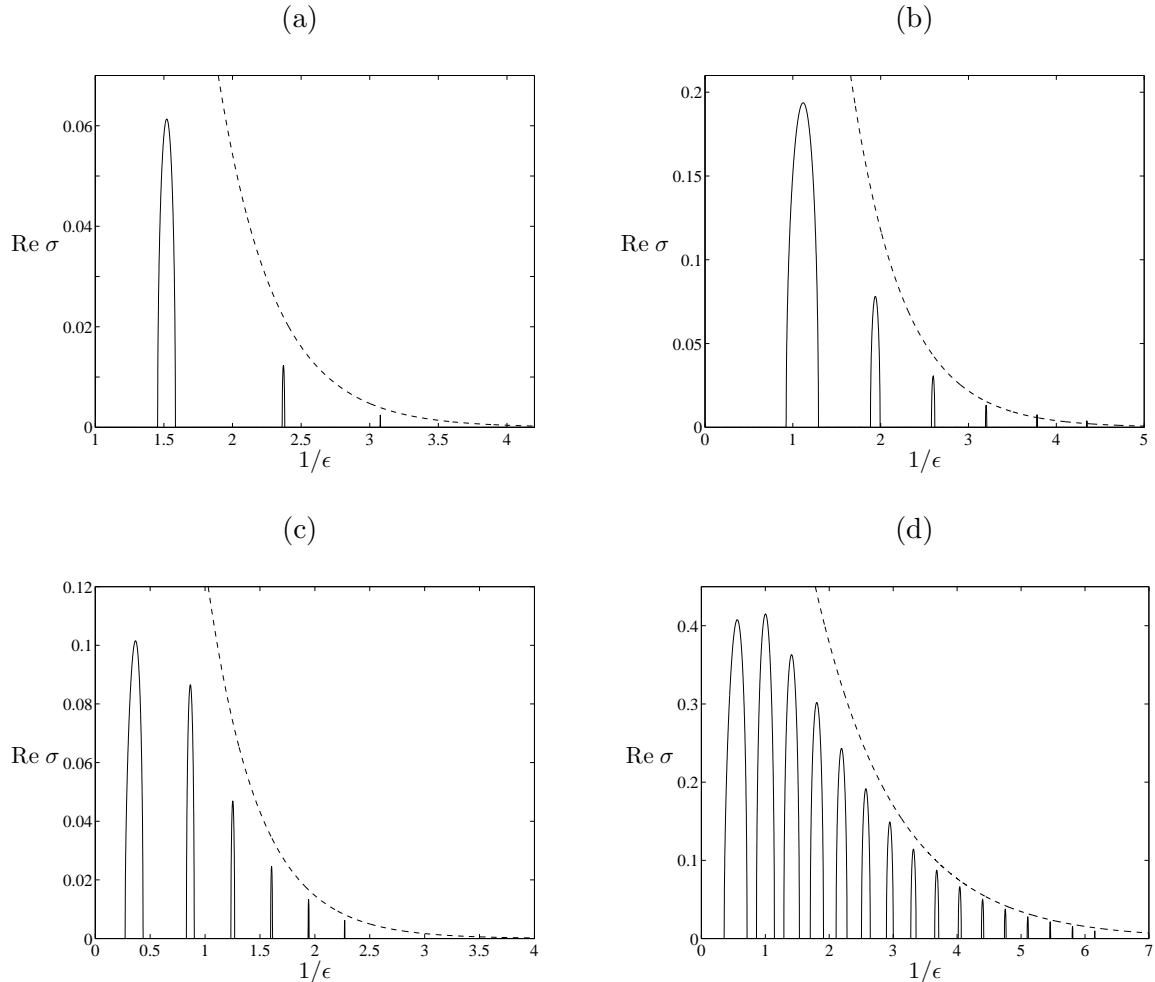


Figure 2: Growth rates $\text{Re } \sigma$ in anticyclonic flows as functions of the inverse Rossby number $1/\epsilon$ for (a) $e = 1.5$, $\mu = 1$; (b) $e = 2$, $\mu = 1$; (c) $e = 2$, $\mu = 0.5$; and (d) $e = 4$, $\mu = 1$. The growth rates computed numerically (solid lines) are compared with the asymptotic estimate of the maximum growth rates σ_{\max} (dashed lines).

Evaluating this quantity for the parameters chosen for the figures gives $\gamma = 0.62$, 0.54 , 0.31 and 0.34 for the parameters of Figure 2 (a)–(d), and $\gamma = 0.18$ and 0.12 for the parameters of Figure 3 (a) and (b), in good agreement with the numerical results.

Our derivation of an asymptotic expression for the growth rate makes the hydrostatic approximation, which assumes that $N \gg f$, $m_0 \gg k_0$ and $\mu = fm_0/(Nk_0) = O(1)$. This assumption, which could be relaxed, is made because it corresponds to the regime most relevant to atmospheric and oceanic flows; it is consistent in the sense that the growth rates obtained are maximized for $\mu = O(1)$ and decay rapidly for $\mu \gg 1$ or $\mu \ll 1$. To test the sensitivity of the

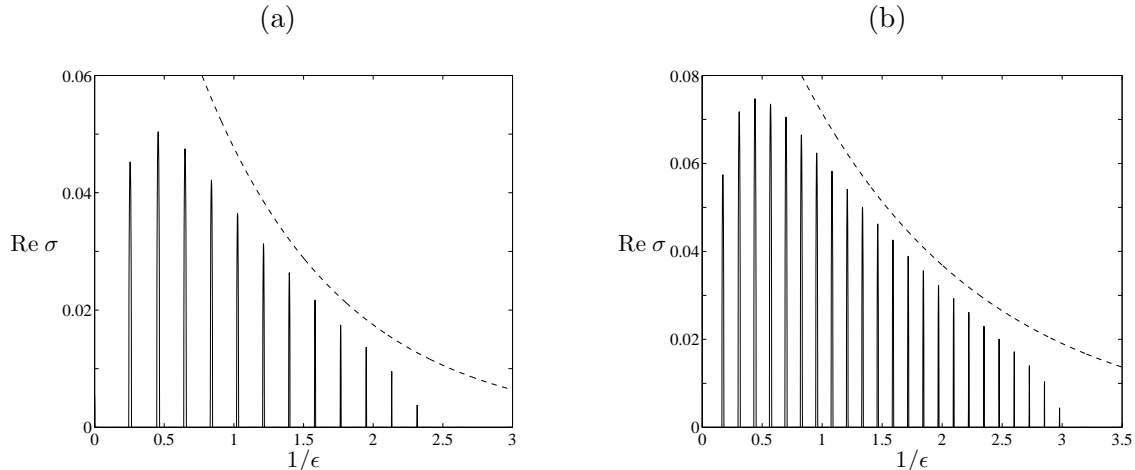


Figure 3: Growth rates $\text{Re } \sigma$ in cyclonic flows as functions of the inverse Rossby number $1/\epsilon$ for (a) $e = 4$, $\mu = 0.5$; and (b) $e = 6$, $\mu = 0.5$. The growth rates computed numerically (solid lines) are compared with the asymptotic estimate of the maximum growth rates σ_{\max} (dashed lines).

results to the hydrostatic approximation, we have solved the Floquet problem numerically for the full, unapproximated equation (2.5) for moderately large values of N/f and m_0/k_0 . The results obtained for $\mu = 1$ and $e = 4$ are displayed in Figure 4. This compares the growth rate obtained in the hydrostatic approximation with those obtained for $N/f = m_0/k_0 = 3$ and 6. Except for $\epsilon \gtrsim 1$, there is relatively little difference between the results: the maximum growth rates fall on the same curve, well described by the hydrostatic asymptotics. Of course, the location of the instability bands changes depending on S , but this is not significant, since they would also change if m_0/k_0 was varied independently of N/f , as is physically relevant.

Acknowledgments. The authors acknowledge the support of the EPSRC Network ‘Wave–Flow Interactions’. JMA is supported by a studentship of the UK Natural Environment Research Council.

A Exponential asymptotics

In this Appendix, we compute the (exponentially small) Stokes multiplier S which quantifies the switching on of one branch of the WKB solution by the other (see (3.5)–(3.6)) through a Stokes phenomenon^{12;16}. The Stokes phenomenon is associated with the presence of complex turning points, that is, complex times where $\omega = 0$. From (2.10), these are located at

$$t_n = i \sinh^{-1} \frac{\sqrt{1 + \mu^2}}{\psi} + n\pi, \quad n = 0, \pm 1, \pm 2, \dots$$

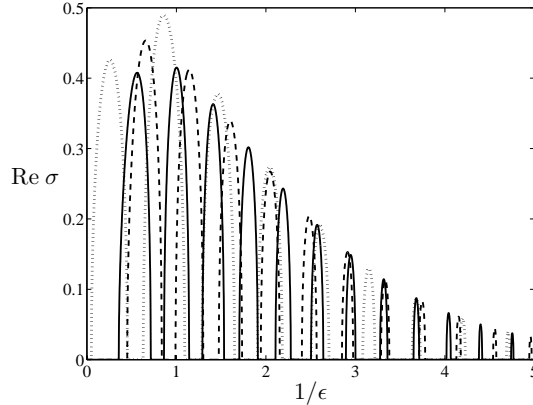


Figure 4: Effect of the hydrostatic approximation: the growth rate $\text{Re } \sigma$ is plotted as a function of the inverse Rossby number $1/\epsilon$ for an anticyclonic flow with $e = 4$ and $\mu = 1$, in the hydrostatic limit $N/f \rightarrow \infty$ (solid lines), for $N/f = 6$ (dashed lines), and for $N/f = 3$ (dotted lines).

and \bar{t}_n . The Stokes phenomenon occurs as $t \in \mathbb{R}$ crosses one of the Stokes lines joining t_n to \bar{t}_n . In the interval $[-\pi/2, \pi/2]$ of interest, the only Stokes line is the segment of $\text{Re } t = 0$ joining t_0 to \bar{t}_0 . We compute S using matched asymptotics, examining how the solution $\zeta = A(t) \exp(i\theta(t)/\epsilon)$ connects to the solution $\zeta = A(t)[\exp(i\theta(t)/\epsilon) + S \exp(-i\theta(t)/\epsilon)]$ as this segment is crossed.¹⁷

To analyse the behaviour of the solution in the neighbourhood of t_0 , we first note that

$$\omega \sim a^{1/2} e^{i\pi/4} (t - t_0)^{1/2}, \quad \text{where } a = \sqrt{2(1 + \mu^2)(1 + \psi^2 + \mu^2)}/\mu^2, \quad (\text{A.1})$$

as $t \rightarrow t_0$. We then rescale the evolution equation for ζ near t_0 by defining the inner variables

$$\tau = \epsilon^{-2/3} a^{1/3} (t - t_0) \quad \text{and} \quad Z(\tau) = \zeta(t).$$

Retaining only the leading order terms, this transforms (2.9) into the equation

$$\frac{d^2 Z}{d\tau^2} + i\tau Z = 0. \quad (\text{A.2})$$

Solutions can be written in terms of the Airy functions $\text{Ai}(e^{-i\pi/6}\tau)$ and $\text{Bi}(e^{-i\pi/6}\tau)$. We claim that the solution of interest is

$$Z \sim C \left[\text{Ai}(e^{-i\pi/6}\tau) + i\text{Bi}(e^{-i\pi/6}\tau) \right]. \quad (\text{A.3})$$

We verify that this solution matches $A(t) \exp(i\theta(t)/\epsilon)$ to the left of the Stokes line $\text{Re } t = 0$; in doing so we find an expression for the constant C . It is convenient to verify the matching along

the line $\text{ph } \tau = -5\pi/6$; this is an anti-Stokes line along which the two independent solutions of (A.2) have similar orders of magnitudes. Along this line, we can use the asymptotic formulas¹⁸

$$\text{Ai}(-z) \sim \frac{1}{\sqrt{\pi}z^{1/4}} \cos(2z^{3/2}/3 - \pi/4), \quad (\text{A.4})$$

$$\text{Bi}(-z) \sim -\frac{1}{\sqrt{\pi}z^{1/4}} \sin(2z^{3/2}/3 - \pi/4), \quad (\text{A.5})$$

with $z = -\exp(-i\pi/6)\tau = \exp(5i\pi/6)\tau \rightarrow +\infty$. Thus we have

$$Z \sim \frac{Ce^{i\pi/24}}{\sqrt{\pi}\tau^{1/4}} e^{2ie^{i\pi/4}\tau^{3/2}/3}. \quad (\text{A.6})$$

On the other hand, using (3.3)–(3.4) the solution $\zeta = A(t) \exp(i\theta(t))$, valid in the outer region away from t_0 and to the left of the Stokes line $\text{Re } t = 0$, can be written as

$$\begin{aligned} \zeta &\sim \frac{1}{\omega^{1/2}} e^{\int_{-\pi/2}^t p(t') dt'/2} e^{i\epsilon^{-1} \int_{-\pi/2}^t [\omega(t') - \epsilon q(t')/(2\omega(t'))] dt'} \\ &\sim \frac{e^{-i\pi/8}}{(\epsilon a)^{1/6} \tau^{1/4}} e^{\int_{\Gamma_-} p(t') dt'/2} e^{i\epsilon^{-1} \int_{\Gamma_-} [\omega(t') - \epsilon q(t')/(2\omega(t'))] dt'} e^{2ie^{i\pi/4}\tau^{2/3}/3}, \end{aligned} \quad (\text{A.7})$$

after using (A.1). Here Γ_- denotes a contour joining $-\pi/2$ to t_0 while remaining to the left of the Stokes line $\text{Re } t = 0$. Comparing (A.7) with (A.6) shows that ζ correctly matches Z provided that

$$C = \frac{\sqrt{\pi}e^{-i\pi/6}}{(\epsilon a)^{1/6}} e^{\int_{\Gamma_-} p(t') dt'/2} e^{i\epsilon^{-1} \int_{\Gamma_-} [\omega(t') - \epsilon q(t')/(2\omega(t'))] dt'}. \quad (\text{A.8})$$

We now match Z with the outer solution valid to the right of the Stokes line $\text{Re } t = 0$. A connection formula for Airy functions¹⁸ gives the alternative form

$$Z \sim 2Ce^{i\pi/3} \text{Ai}(e^{-i5\pi/6}\tau), \quad (\text{A.9})$$

for (A.3). Carrying out the matching on the anti-Stokes line $\text{ph } \tau = \exp(-i\pi/6)$, we can use the asymptotic formula for Ai in (A.4) to write that

$$Z \sim \frac{Ce^{i\pi/24}}{\sqrt{\pi}\tau^{1/4}} \left(e^{2ie^{i\pi/4}\tau^{3/2}/3} + ie^{-2ie^{i\pi/4}\tau^{3/2}/3} \right) \quad (\text{A.10})$$

for $|\tau| \rightarrow \infty$. This should be matched with the form $\zeta(t) = A(t)[\exp(i\theta(t)/\epsilon) + S \exp(-i\theta(t)/\epsilon)]$ of the solution to the right of the Stokes line. Using (A.1) gives the asymptotics

$$\begin{aligned} \zeta &\sim \frac{1}{\omega^{1/2}} e^{\int_{-\pi/2}^t p(t') dt'/2} \left[e^{i\epsilon^{-1} \int_{-\pi/2}^t [\omega(t') - \epsilon q(t')/(2\omega(t'))] dt'} + S e^{-i\epsilon^{-1} \int_{-\pi/2}^t [\omega(t') - \epsilon q(t')/(2\omega(t'))] dt'} \right] \\ &\sim \frac{e^{-i\pi/8}}{(\epsilon a)^{1/6} \tau^{1/4}} e^{\int_{\Gamma_+} p(t') dt'/2} \left[e^{i\epsilon^{-1} \int_{\Gamma_+} [\omega(t') - \epsilon q(t')/(2\omega(t'))] dt'} e^{2ie^{i\pi/4}\tau^{3/2}/3} \right. \\ &\quad \left. + S e^{-i\epsilon^{-1} \int_{\Gamma_+} [\omega(t') - \epsilon q(t')/(2\omega(t'))] dt'} e^{-2ie^{i\pi/4}\tau^{3/2}/3} \right], \end{aligned}$$

where Γ_+ denotes a contour joining $-\pi/2$ to t_0 . This contour crosses the Stokes line $\text{Re } t = 0$ below the singular point t_p of $p(t)$ and $q(t)$, given by $t_p = \text{isinh}^{-1}(1/\psi)$. Taking (A.8) into account, the matching with (A.10) gives the two equations

$$\begin{aligned} e^{\int_{\Gamma_-} p(t) dt/2} e^{-i \int_{\Gamma_-} q(t)/\omega(t) dt/2} &= e^{\int_{\Gamma_+} p(t) dt/2} e^{-i \int_{\Gamma_+} q(t)/\omega(t) dt/2}, & (\text{A.11}) \\ i e^{\int_{\Gamma_-} p(t') dt'/2} e^{i\epsilon^{-1} \int_{\Gamma_-} [\omega(t') - \epsilon q(t')/(2\omega(t'))] dt'} &= S e^{\int_{\Gamma_+} p(t') dt'/2} e^{-i\epsilon^{-1} \int_{\Gamma_+} [\omega(t') - \epsilon q(t')/(2\omega(t'))] dt'} \end{aligned} \quad (\text{A.12})$$

We can now deform the integration contours. The difference $\int_{\Gamma_+} - \int_{\Gamma_-}$ reduces to an integral along a closed contour encircling t_p . Computing the corresponding residues using (2.11) gives

$$\text{Res}_{t_p} p = 1 \quad \text{and} \quad \text{Res}_{t_p} \frac{q}{\omega} = -i\varsigma,$$

Taking this into account confirms that (A.11) is an identity. Using $\text{Res}_{t_p} p = 1$ in (A.12) gives the Stokes multiplier as

$$S = -i e^{2i\epsilon^{-1} \mathcal{P} \int_{-\pi/2}^{t_0} [\omega(t') - \epsilon q(t')/(2\omega(t'))] dt'},$$

where the Cauchy principal value integral, denoted by \mathcal{P} , is necessary because $q(t)$ has a pole at $t = t_p$. It follows that $|S|$, giving the instability growth rate, can be written as

$$|S| = e^{-\alpha/\epsilon + \varsigma\beta},$$

where the two constants

$$\alpha = -2i \int_0^{t_0} \omega(t) dt \quad \text{and} \quad \beta = -i \mathcal{P} \int_0^{t_0} \frac{\varsigma q(t)}{\omega(t)} dt$$

are real, positive and independent of ς . Using (2.10) and (2.11), they can be given the more explicit forms

$$\alpha = \frac{2}{\mu} \int_0^{\text{sinh}^{-1}(\sqrt{1+\mu^2}/\psi)} \sqrt{1 - \psi^2 \sinh^2 u + \mu^2} du,$$

and

$$\beta = \mu\varsigma \int_0^{\text{sinh}^{-1}(\sqrt{1+\mu^2}/\psi)} \left(e + e^{-1} + \frac{2e}{1 - \psi^2 \sinh^2 u} \right) \frac{du}{\sqrt{1 - \psi^2 \sinh^2 u + \mu^2}},$$

and further transformed into the convenient expressions (3.12)–(3.13).

References

- [1] R. R. Kerswell. Elliptical instability. *Ann. Rev. Fluid Mech.*, 34:83–113, 2002.
- [2] T. Miyazaki. Elliptical instability in a stably stratified rotating fluid. *Phys. Fluids*, A 5: 2702–2709, 1993.

- [3] J. C. McWilliams and I. Yavneh. Fluctuation growth and instability associated with a singularity of the balance equations. *Phys. Fluids*, 10:2587–2596, 1998.
- [4] M. J. Molemaker, J. C. McWilliams, and I. Yavneh. Baroclinic instability and loss of balance. *J. Phys. Oceanogr.*, 35:1505–1517, 2005.
- [5] J. Vanneste and I. Yavneh. Unbalanced instabilities of rapidly rotating stratified shear flows. *J. Fluid Mech.*, 584:373–396, 2007.
- [6] J. C. McWilliams, M. J. Molemaker, and I. Yavneh. Ageostrophic, anticyclonic instability of a geostrophic, barotropic boundary current. *Phys. Fluids*, 16:3720–3725, 2004.
- [7] R. Plougonven, D. J. Muraki, and C. Snyder. A baroclinic instability that couples balanced motions and gravity waves. *J. Atmos. Sci.*, 62:1545–1559, 2005.
- [8] J. Vanneste and I. Yavneh. Exponentially small inertia-gravity waves and the breakdown of quasi-geostrophic balance. *J. Atmos. Sci.*, 61:211–223, 2004.
- [9] J. Vanneste. Exponential smallness of inertia-gravity-wave generation at small Rossby number. *J. Atmos. Sci.*, 65:1622–1637, 2008.
- [10] C. M. Bender and S. A. Orszag. *Advanced mathematical methods for scientists and engineers*. Springer, 1999.
- [11] M. I. Weinstein and J. B. Keller. Asymptotic behaviour of stability regions for Hill’s equation. *SIAM J. Appl. Math.*, 47:941–958, 1987.
- [12] M. J. Ablowitz and A. S. Fokas. *Complex variables: introduction and applications*. Cambridge University Press, 1997.
- [13] S. J. Friedlander and A. Lipton-Lifschitz. Localized instabilities in fluids. In S.J. Friedlander and D. Serre, editors, *Handbook of Mathematical Fluid Dynamics, vol. II*, pages 289–353. Elsevier Science, 2003.
- [14] S. Le Dizès. Three-dimensional instability of a multipolar in a rotating flow. *Phys. Fluids*, 12:2762–2774, 2000.
- [15] R. C. Kloosterziel, G. F. Carnevale, and P. Orlandi. Inertial instability in rotating stratified fluids: barotropic vortices. *J. Fluid Mech.*, 583:379–412, 2007.

- [16] R. B. Paris and A. D. Wood. Stokes phenomenon demystified. *Bull. Inst. Math. Appl.*, 31: 21–28, 1995.
- [17] V. Hakim. Asymptotic techniques in nonlinear problems: some illustrative examples. In C. Godrèche and P. Manneville, editors, *Hydrodynamics and nonlinear instabilities*, chapter 3, pages 295–386. Cambridge University Press, 1998.
- [18] M. Abramowitz and I. A. Stegun. *Handbook of mathematical functions*. Dover, 1965.

